Overcoming hERG issues for brain-penetrating cathepsin S inhibitors: 2-Cyanopyrimidines. Part 2

Osamu Irie [a,*], Takatoshi Kosaka [a], Masashi Kishida [a], Junichi Sakaki [a], Keiichi Masuya [a], Kazuhide Konishi [a], Fumiaki Yokokawa [a], Takeru Ehara [a], Atsuko Iwasaki [a], Yuki Iwaki [a], Yuko Hitomi [a], Atsushi Toyao [a], Hiroki Gunji [a], Naoki Teno [a], Genji Iwasaki [a], Hajime Hirao [a], Takanori Kanazawa [a], Keiko Tanabe [a], Peter C. Hiestand [b], Marzia Malcangio [c], Alyson J. Fox [c,†], Stuart J. Bevan [c], Mohammed Yaqoob [c,†], Andrew J. Culshaw [c,†], Terance W. Hart [c], Allan Hallett [c]

[a] Global Discovery Chemistry, Novartis Institutes for BioMedical Research, Ohkubo 8, Tsukuba, Ibaraki 300-2611, Japan
[b] Novartis Institutes for BioMedical Research, Basel CH-4002, Switzerland
[c] Novartis Institutes for BioMedical Research, 5 Gower Place, London WC1E 6BS, UK

ARTICLE INFO

ABSTRACT

We describe here orally active and brain-penetrant cathepsin S selective inhibitors, which are virtually devoid of hERG K⁺ channel affinity, yet exhibit nanomolar potency against cathepsin S and over 100-fold selectivity to cathepsin L. The new non-peptidic inhibitors are based on a 2-cyanopyrimidine scaffold bearing a spiro[3.5]non-6-yl-methyl amine at the 4-position. The brain-penetrating cathepsin S inhibitors demonstrate potential clinical utility for the treatment of multiple sclerosis and neuropathic pain.

Cathepsin S (Cat S) is a cysteine protease predominantly expressed in dendritic cells, B cells, macrophages, and brain microglia. In these antigen presenting cells Cat S plays an essential role in the proteolytic events that lead to antigen presentation at the cells surface for recognition by T cells.[1] In addition, Cat S can be secreted by activated microglia and might play a role in regulating extra cellular matrix interaction.[2] We have recently demonstrated that inhibition of spinal microglial Cat S reversed neuropathic pain.[3] It was also reported that in Creutzfeldt–Jakob disease (CJD) infected mice Cat S expression has been increased, which could result from microglia cell activation.[4] Cat S might be involved in multiple sclerosis (MS), myasthenia gravis (MG), Alzheimer's disease (AD), and Down disease.[5] These findings suggest that a Cat S inhibitor which penetrates blood–brain barrier (BBB) could be beneficial for various brain diseases. Herein, we describe the discovery of non-peptidic Cat S inhibitors having a balanced blood–brain penetration after overcoming a human ether-a-go-go-related gene (hERG) K⁺ channel blocking issue which has often been observed in central nervous system (CNS) drugs.[6]

We have recently reported a novel class of Cat S inhibitor **1**, the 4,5,6-trisubstituted 2-cyanopyrimidine derivatives (Fig. 1).[7] However, the selectivity against the off-target enzyme, Cat L was insufficient to reach the clinical phase. Cat L deficient mice develop periodic hair loss and epidermal hyperplasia, indicating that Cat L is essential for epidermal homeostasis and regular hair follicle morphogenesis and cycling.[8] Our next focus was thus on improv-
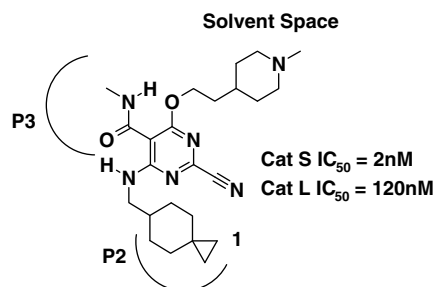

Figure 1. The 4,5,6-trisubstituted pyrimidine scaffold for Cat S inhibitors.

---

* Corresponding author. Tel.: +81 29 865 2384; fax: +81 29 865 2308.
  E-mail addresses: osamu.irie@novartis.com, o.irie1@d4.dion.ne.jp (O. Irie).
† Present address: Novartis Horsham Research Center, Wimblehurst Road, Horsham RH12 5AB, UK.

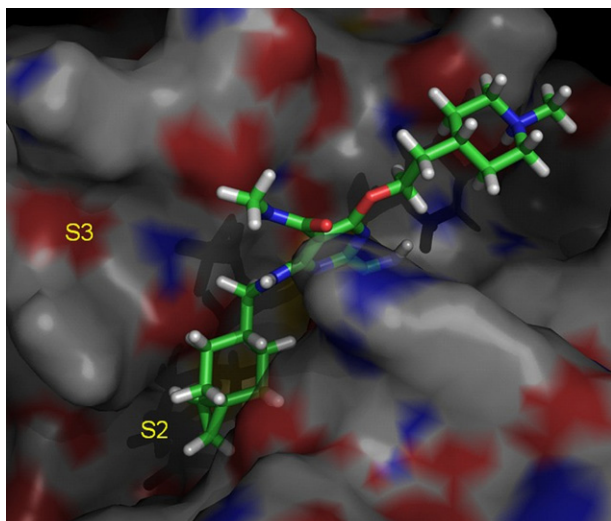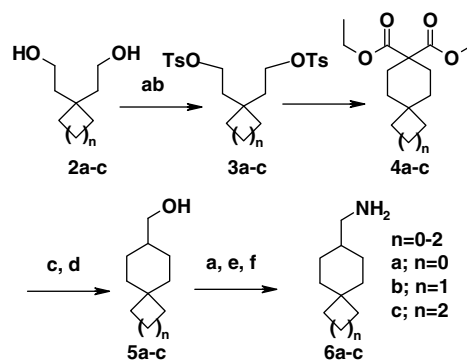**Figure 2.** Compound **1** docked with human Cat S.

Scheme 1. Reagents and conditions: (a) TsCl, NMe₃-HCl, NEt₃, CH₂Cl₂, 0 °C, 1 h, quant.; (b) CH₂(CO₂Et)₂, NaH, THF, rt–60 °C, 3 h; (c) LiCl, H₂O, DMSO, 185 °C, 10 h, 48–59% (3 steps); (d) LiAlH₄, THF, 0 °C, 0.5 h, 82–84%; (e) NaN₃, DMF, rt, 0.5 h; (f) PPh₃, THF–H₂O, rt, 23 h, 73–75% (2 steps).

ing the selectivity of Cat S inhibitors against Cat L by modifying the P2 moiety of **1**, which interacts with the S2 subsite of each cathepsin, a key pocket for controlling the selectivity of cathepsin inhibitors.[7]

The X-ray crystal structures of human Cat S (PDB code 1MS6) and Cat L (PDB code 3BC3) suggested that the S2 subsite of the Cat S enzyme accepts a slightly larger group than that for Cat L.[9,10] The bottom of the S2 subsite in the Cat S enzyme has Gly137 and Gly165, while the corresponding region in Cat L comprises of Ala135 and Gly164. Our computer-assisted modeling studies concluded that the S2 pocket of Cat S would accommodate

a slightly bulkier P2 group than the spiro[2.5]oct-6-yl-methyl amine group of compound **1** (Fig. 2).

The spiro amine syntheses are shown in Scheme 1. Treatment of 2-[1-(2-hydroxy-ethyl)-cycloalkyl]-ethanol **2a–c**[11] with tosylchloride, triethylamine, and a catalytic amount of trimethylamine hydrochloride[12] in CH₂Cl₂ afforded ditosylate **3a–c**. Cyclization of **3a–c** with diethyl malonate under basic conditions in THF provided spiro diesters **4a–c**. Decarboxylation reaction of **4a–c** with lithium chloride and water in DMSO at 185 °C, followed by reduction of the resulting esters by LiAlH₄, gave spiro alcohols **5a–c** which were converted to amines **6a–c** by treatment of the tosylates with sodium azide in DMF following by azide reduction with PPh₃ in THF–H₂O.

We used a multi-parallel synthesis approach for the optimization of the 4- and 6-substituents on the 2-cyanopyrimidine by
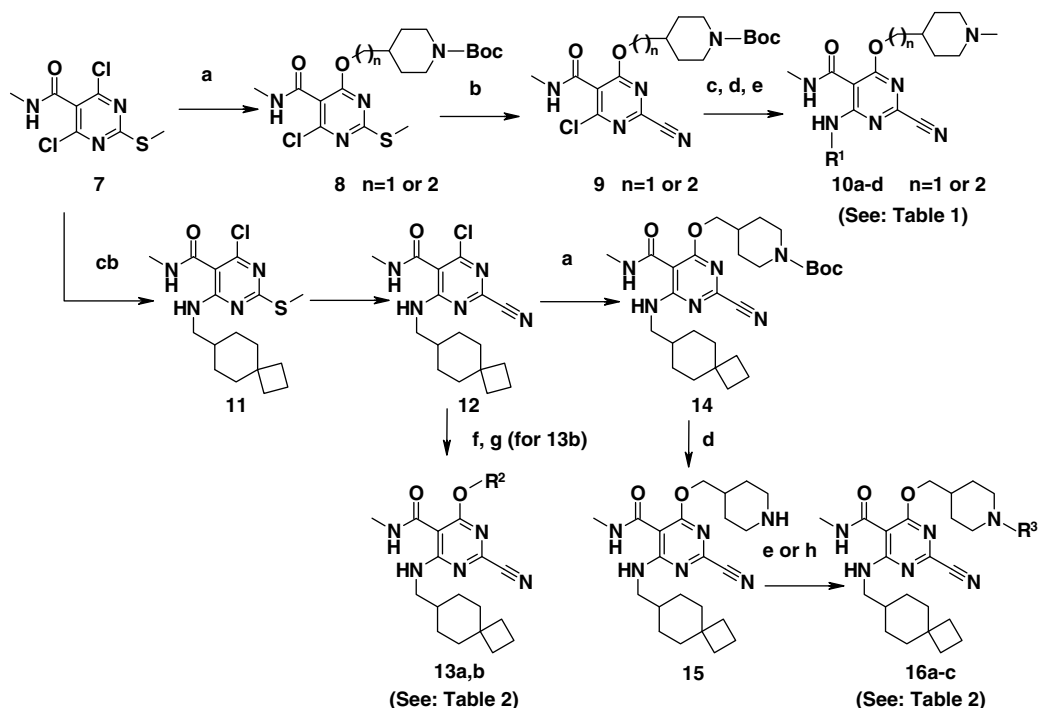
Scheme 2. Reagents and conditions: (a) HO(CH₂)ₙ(4-piperidine-N-Boc), NaH, THF, 0–60 °C, 6 h, 52–97%; (b) i—mCPBA, NaHCO₃, CH₂Cl₂, 0 °C–rt, 10 h; ii—KCN, nBu₄N⁺Br⁻, 18-Crown-6, CH₂Cl₂–H₂O, rt, 3 h, 41–66% (2 steps); (c) R¹-NH₂, NEt₃, THF, 0 °C–rt, 90–99%.; (d) 4 mol/L HCl–AcOEt, rt, 0.5 h, quant. or TFA, CH₂Cl₂ (for **10c**, **10e**), rt, 10 min, 30–34%; (e) HCHO or acetone, NaBH₃(CN), AcOH, THF, 0 °C–rt, 1.5 h, 38–58%; (f) HO(CH₂)₂OTHP, or 2,2,6,6-tetramethylpiperidine-4-ol, NaH, THF, 0–60 °C, 6 h, 82–99%; (g) PPTS, EtOH, 70 °C, 6 h, 69–78%; (h) Br(CH₂)₂OH, K₂CO₃, DMF, 0 °C–rt, 12 h, 49%, or AcCl, NEt₃, CH₂Cl₂, 0 °C–rt, 12 h, 71%.

using compounds **9** and **12** in Scheme 2 as key intermediates. Condensation of 4,6-dichloro-2-methylsulfanyl-pyrimidine-5-carboxylic acid methylamide **7**[7] with N-Boc-piperazine-4-methanol or ethanol under the basic conditions in THF afforded **8a**, **b**. Conversion of the methyl sulfides to nitriles **9** was performed by oxidation with mCPBA followed by treatment with potassium cyanide. Treatment of the key intermediate **9** with amines **6a–c**, the commercially available cyclopentylethylamine, or C-(1,4-dioxaspiro[4.5]dec-8-yl)-methylamine[13], followed by deprotection of the Boc group and reductive amination with HCHO and NaBH$_3$(CN), provided the desired compounds **10a–d**.

The synthesis for the optimization of the 6-substituent on the 2-cyanopyrimidine is also described in Scheme 2. Condensation of **7** and C-spiro[3.5]non-7-yl-methylamine **6b** gave compound **11** which was converted to a 6-chloro-2-cyanopyrimidine intermediate **12**. Addition of 2,2,6,6-tetramethylpiperidine-4-ol or 2-(tetrahydropyran-2-yloxy)-ethanol with sodium hydride in THF, followed by deprotection under acidic conditions provided the desired compounds **13a**, **b**. Condensation of **12** with N-Boc-piperidine 4-methanol and subsequent treatment with 4 mol/L HCl solution in ethyl acetate or trifluoroacetic acid afforded the secondary amine **15**. N-Substitution of the piperazine in **15** by acylation, reductive amination, or by using alkyl halides provided tertiary amines **16a–c**.
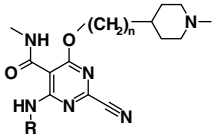
The results of the SAR study on the optimization of the P2 moiety are described in Table 1. Expansion of the spiro ring at the end of P2 by replacement of the spirocyclopropyl with cyclobutyl group improved selectivity against Cat L (Table 1; **1** vs **10a**). However, further expansion of the spiro ring decreased both potency and selectivity toward Cat S (**10b** vs **10d**). Introduction of a polar functional group on the P2 part was not tolerated because of the hydrophobic natures of the S2 subsites in both Cat S and Cat L (**10b** vs

10c).[14] In summary of P2 moiety, the spiro[3.5]non-6-yl-methyl amine **6a** was an optimum size for P2 based on the balance of potency and selectivity to Cat S.

In the past decade, a number of drugs failed to reach or were withdrawn from the market due to cardiosafety issues. It is now widely known that inhibition of hERG K$^+$ channel is one of the major causes of the observed cardiac side effects, which are drug-induced QT prolongation and/or arrhythmia called Torsades de Pointes. Our designed Cat S inhibitors **10a**, **b** showed unacceptable affinity to the hERG K$^+$ channel as indicated by the binding assay using [^{3}H]dofetilide. We thus needed to decrease the hERG K$^+$ channel binding affinity of compounds by modification of the 6-substituent on the 2-cyanopyrimidine. Introduction of many functional groups at the pyrimidine 6-position could be well tolerated by the Cat S active site, as the 6-substituent orients itself toward the solvent space in the modeling (Fig. 2). Indeed, all compounds in Table 2 having a variety of substituents at the pyrimidine 6-position, showed excellent inhibitory activity and selectivity toward Cat S. A SAR study of the 2-cyanopyrimidines on the hERG K$^+$ channel binding affinity is shown in Table 2.

A typical 3D pharmacophore model for prediction of hERG K$^+$ channel binding activity has been published.[6,18] The model suggests that the classic hERG K$^+$ channel blocker motif contains a basic nitrogen center flanked by an aromatic or hydrophobic group. We thus attempted to modulate the basicity of the piperidine ring in the 6-substituent on the 2-cyanopyrimidine core. Decreasing the basicity of the nitrogen atom by replacing the tertiary amine with a secondary amine decreased the hERG binding activity (Table 2; **10b** vs **15**). An increase in basicity by replacement of N-methyl piperidine by N-isopropyl piperidine showed the anticipated increase in affinity to the hERG K$^+$ channel (**16a**, hERG
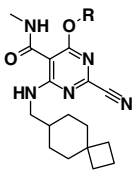
Table 1
Optimization of the P2 moiety

Compound	n	R	IC$_{50}$ (nM)[a]		
			Cat S	Cat L	hERG[b]
1	2	-CH$_2$ (spirocyclopropyl)	2	120	NT[c]
10a	2	-CH$_2$ (spirocyclobutyl)	4	440	420
10b	1	-CH$_2$ (spirocyclobutyl)	3	360	710
10c	1	-CH$_2$ (dioxolane spiro)	>1000	>1000	NT[c]
10d	1	-CH$_2$ (spirocyclopentyl)	12	276	1455
10e	1	-CH$_2$ (dioxolane)	31	426	5770
10d	1	-(CH$_2$)$_2$ (cyclopentyl)	26	400	360

[a] Inhibition profiles were determined by a fluorometric assay with recombinant human Cat L and Cat S, employing Z-Phe-Arg-AMC (Cat L) and L-Leu-Leu-Arg-AMC (Cat S) as synthetic substrates.[15] Data represent means of two experiments performed in duplicate. Individual data points in each experiment were within a twofold range with each other.
[b] Inhibition profiles were determined by a radioligand binding assay with [^{3}H]dofetilide binding to a crude membrane preparation of HEK293 cell membranes stably transfected with hERG channels.[16]
[c] NT, not tested.

Table 2
Optimization of the 6 position on the pyrimidine ring[17]

Compound	R	IC$_{50}$ (nM)[a]		
		Cat S	Cat L	hERG[b]
10b	-CH$_2$ (piperidine N—)	3	360	710
16a	-CH$_2$ (piperidine N-isopropyl)	3	330	540
16b	-CH$_2$ (piperidine N-CH$_2$CH$_2$OH)	3	300	890
15	-CH$_2$ (piperidine NH)	5	460	2340
13a	(tetramethylpiperidine NH)	5	1390	5040
16c	-CH$_2$ (piperidine N-acetyl)	10	2500	>30,000
13b	-CH$_2$CH$_2$OH	6	1200	>30,000

[a] Inhibition profiles were determined by a fluorometric assay with recombinant human Cat K, L, and S, employing Z-Phe-Arg-AMC (Cat K and L) and L-Leu-Leu-Arg-AMC (Cat S) as synthetic substrates.[15] Data represent means of two experiments performed in duplicate. Individual data points in each experiment were within a twofold range with each other.
[b] Inhibition profiles were determined by a radioligand assay with [^{3}H]dofetilide binding to a crude membrane preparation of HEK293 cell membranes stably transfected with hERG channels.[16]

Table 3
Plasma and brain concentration profiles for several compounds in Sprague–Dawley rats (po 10 mg/kg), where values are means of $n = 3$

Compound	Plasma concentration (nM)		Brain concentration (nM)	
	1 h	3 h	1 h	3 h
10b	346	308	124	718
16a	191	381	67	455
15	28	61	<13	<13
13a	–	287	–	164
16c	169	80	27	<13
13b	283	170	692	849

Table 4
Pharmacokinetic parameters of **10b**, **16a**, and **13b** in male Sprague–Dawley rats (iv 1 mg/kg; po 10 mg/kg), where values are means of $n = 3$

Compound	$_{po}C_{max}$ (nM)	Cl_p (L/h/ kg)	$_{iv}t_{1/2}$ (h)	F (%)	$_{po}$ AUC (nM h)	V_{dss} (L/ kg)
10b	461	1.1	6.7	40	8237	9.8
16a	298	0.6	11.8	24	8083	9.3
13b	907	1.5	1.5	14	2503	1.2
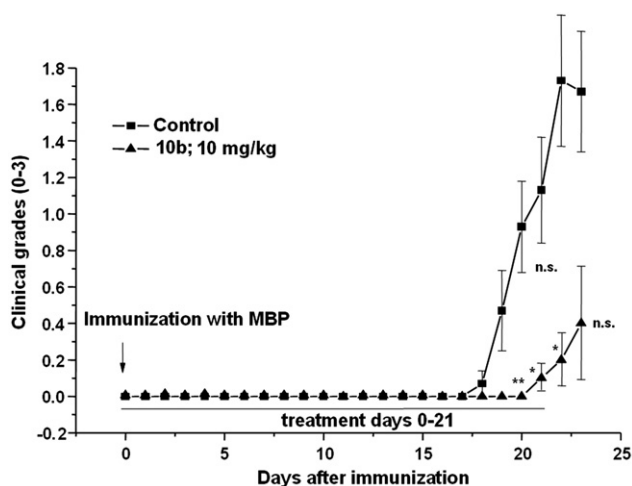
Figure 3. Effect[21] of compound **10b** in acute experimental autoimmune encephalomyelitis in SJL/J mice. Data presented are means ± SEM. Kruskal–Wallis nonparametric ANOVA, followed by Dunn's multiple comparison test $^*p < 0.05$, $^{**}p < 0.01$ Disease incidence was analyzed using Fisher's exact test (2 × 2 contingency table, 2-sided p value). $n = 15$. MBP, myelin basic protein.

$IC_{50} = 540$ nM). Interestingly, a less basic substituent afforded by N-acylation dramatically decreased the hERG K$^+$ channel binding

affinity (**16a** vs **16c**). Removal of the nitrogen atom by replacement of the piperidine ring with ethyl alcohol also showed significantly attenuated hERG activity (IC_{50} = >30 μM) whilst retaining both potency and selectivity to Cat S (**13b**, Cat S IC_{50} = 6 nM).

We then turned our attention to the CNS penetration of the Cat S inhibitors, which was assessed by following oral administration in rats. The results of the CNS penetration assays are shown in Table 3. The secondary amine **15** and N-acyl piperidine **16c** did not penetrate the BBB in rats, whilst the sterically hindered secondary amine **13a** showed CNS penetration. A tertiary amine also facilitated brain penetration (Table 3; **10b**, **16a**) although these compounds also showed high hERG K$^+$ channel binding affinity. The 6-(2-hydroxy ethoxy) 2-cyanopyrimidine compound **13b** rapidly penetrated the BBB without hERG K$^+$ channel affinity at 30 μM.

The pharmacokinetics (PK) parameters were determined for selected compounds in Sprague–Dawley rats. Representative PK results are shown in Table 4. After intravenous administration compounds, **10b**, **16a**, and **13b** were distributed with the V_{dss} of 1.2–9.8 L/kg and eliminated with the apparent half-lives of 1.5–11.8 h. The maximum plasma concentration (C_{max}) values of the compounds after oral administration were 298–907 nM and the estimated bioavailabilities (F) ranged from 14% to 40%.

Having developed both orally active and brain-penetrating Cat S inhibitors, we next turned to evaluate in vivo efficacy. Multiple sclerosis (MS) is a chronic demyelinating disease of the CNS characterized by scarring plaques distributed along the intracerebral white matter and the spinal cord. The most suitable model of MS is experimental autoimmune encephalomyelitis (EAE) that has well-defined immunologic and genetic profiles for the murine system.[19] We thus evaluated the effect of **10b** on the induction of the acute phase of the chronic progressive form of EAE in SJL/J mice.[20] Oral administration of **10b** (10 mg/kg) twice a day for 21 days prevented the onset of the acute phase of the chronic progressive form of EAE (Fig. 3). These data suggest that brain-penetrating Cat S inhibitors might be useful for the treatment of MS.

We also evaluated the anti-neuropathic pain effect of the developed Cat S inhibitors **10b** and **13b** in Wister rats following oral administration.[3] Both compounds reversed established mechanical hyperalgesia in a dose dependent fashion. The activities of **10b** and **13b** were producing up to 50% reversal of the hyperalgesia (Fig. 4). Following twice daily administration for 5 days, the anti-hyperalgesic activity of the first dose of **13b** (30 mg/kg) against neuropathic hyperalgesia was maintained without serious side effect (Fig. 5). These findings suggest that Cat S inhibition has great promise as a new therapeutic treatment for neuropathic pain.

In summary, we discovered brain-penetrating Cat S inhibitors with nanomolar potency against Cat S, over 100-fold selectivity against Cat L, and excellent PK profiles after overcoming a hERG
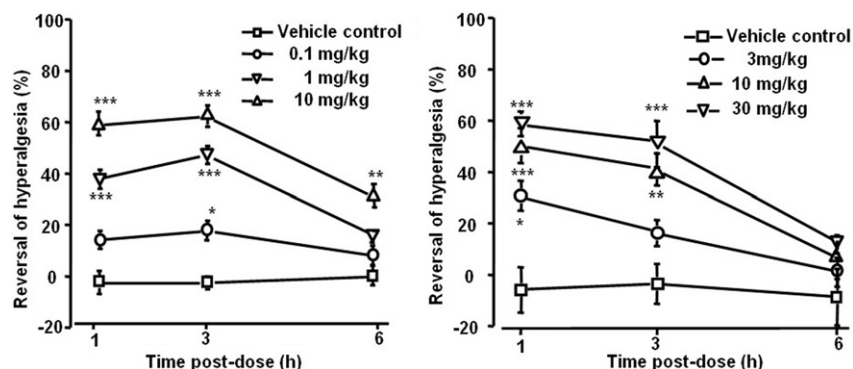
Figure 4. Oral activity of compound **10b** (left) and **13b** (right) against neuropathic mechanical hyperalgesia in rats. Graph depicts mean ± SEM reversal of hyperalgesia from six animals per treatment group. $^{***}p < 0.001$, $^{**}p < 0.01$, $^*p < 0.05$ compared to vehicle by ANOVA followed by Tukey's HSD test carried out on withdrawal threshold data.
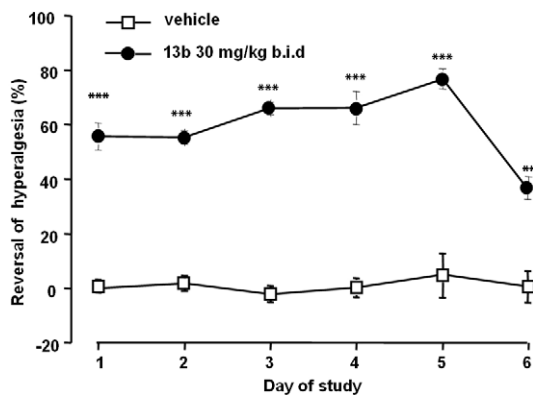
Figure 5. Effect of repeated administration of **13b** on neuropathic pain in rats. Compound **13b** was administered orally in 0.5% methylcellulose/water twice daily for 5 days. Paw withdrawal thresholds were measured 3 h following administration. Each point represents mean ± SEM from 6 animals/group. [***]$p < 0.001$, [**]$p < 0.01$, [*]$p < 0.05$ compared to vehicle by ANOVA followed by Tukey's HSD test.

K^+ channel binding issue by modeling the basicity of the 6-substituent on the 2-cyanopyrimidine core. The compounds demonstrated in vivo activity for MS and neurophatic pain in rodents. We believe that brain-penetrating Cat S inhibitors might be useful for the treatment of these diseases and various other CNS disorders, e.g., AD, CJD, and MG.

Acknowledgments

References and notes

1. Riese, R. J.; Mitchell, R. N.; Villadangos, J. A.; Shi, G.-P.; Palmer, J. T.; Karp, E. R.; De Sanctis, G. T.; Ploegh, H. L.; Chapman, H. A. *J. Clin. Invest.* **1998**, *101*, 2351.
2. Liuzzo, J. P.; Petanceska, S. S.; Moscatelli, D.; Devi, L. A. *Mol. Med.* **1999**, *5*, 320.
3. (a) Clark, A. K.; Yip, P. K.; Grist, J.; Gentry, C.; Staniland, A. A.; Marchand, F.; Dehvari, M.; Wotherspoon, G.; Winter, J.; Ullah, J.; Bevan, S.; Malcangio, M. *Proc. Natl. Acad. Sci. U.S.A.* **2007**, *104*, 10655; (b) Barclay, J.; Clark, A. K.; Ganju, P.; Gentry, C.; Patel, S.; Wotherspoon, G.; Buxton, F.; Song, C.; Ullah, J.; Winter, J.; Fox, A.; Bevan, S.; Malcangio, M. *Pain* **2007**, *130*, 225.
4. Baker, C. A.; Martin, D.; Manuelidis, L. *J. Virol.* **2002**, *76*, 10905.
5. For recent reviews of cathepsin S, see: (a) Berdowska, I. *Clin. Chim. Acta* **2004**, *342*, 41; (b) Gupta, S.; Singh, R. K.; Dastidar, S.; Ray, A. *Expert Opin. Ther. Targets* **2008**, *12*, 291; (c) Maryanoff, B. E.; Costanzo, M. J. *Bioorg. Med. Chem.* **2008**, *16*, 1562; For increased expression of Cat S in hippocampal microglia following kainite-induced seizures, see: (d) Akahoshi, N.; Murashima, Y. L.; Himi, T.; Ishizaki, Y.; Ishii, I. *Neurosci. Lett.* **2007**, *429*, 136.
6. (a) Shipe, W. D.; Barrow, J. C.; Yang, Z.-Q.; Lindsley, C. W.; Yang, F. V.; Schlegel, K.-A. S.; Shu, Y.; Rittle, K. E.; Bock, M. G.; Hartman, G. D.; Tang, C.; Ballard, J. E.; Kuo, Y.; Adarayan, E. D.; Prueksaritanont, T.; Zrada, M. M.; Uebele, V. N.; Nuss,

C. E.; Connolly, T. M.; Doran, S. M.; Fox, S. V.; Kraus, R. L.; Marino, M. J.; Graufelds, V. K.; Vargas, Hu M.; Bunting, P. B.; Hasbun-Manning, M.; Evans, R. M.; Koblan, K. S.; Renger, J. J. *J. Med. Chem.* **2008**, *51*, 3692; (b) Yoshizumi, T.; Miyazoe, H.; Ito, H.; Tsujita, T.; Takahashi, H.; Asai, M.; Ozaki, S.; Ohta, H.; Okamoto, O. *Bioorg. Med. Chem. Lett.* **2008**, *18*, 3778; (c) Yoshizumi, T.; Takahashi, H.; Miyazoe, H.; Sugimoto, Y.; Tsujita, T.; Kato, T.; Ito, H.; Kawamoto, H.; Hirayama, M.; Ichikawa, D.; Azuma-Kanoh, T.; Ozaki, S.; Shibata, Y.; Tani, T.; Chiba, M.; Ishii, Y.; Okuda, S.; Tadano, K.; Fukuroda, T.; Okamoto, O.; Ohta, H. *J. Med. Chem.* **2008**, *51*, 4021; (d) Kawai, M.; Ando, K.; Matsumoto, Y.; Sakurada, I.; Hirota, M.; Nakamura, H.; Ohta, A.; Sudo, M.; Hattori, K.; Takashima, T.; Hizue, M.; Watanabe, S.; Fujita, I.; Mizutani, M.; Kawamura, M. *Bioorg. Med. Chem. Lett.* **2007**, *17*, 5558; For a recent review on hERG, see: (e) Thai, K.-M.; Ecker, G. F. *Curr. Med. Chem.* **2007**, *14*, 3003.
7. Irie, O.; Yokokawa, F.; Ehara, T.; Iwasaki, A.; Iwaki, Y.; Hitomi, Y.; Konishi, K.; Kishida, M.; Toyao, A.; Masuya, K.; Gunji, H.; Sakaki, J.; Iwasaki, G.; Hirao, H.; Kanazawa, T.; Tanabe, K.; Kosaka, T.; Hart, W. T.; Hallett, A. *Bioorg. Med. Chem. Lett.* **2008**, *18*, 4642.
8. Roth, W.; Deussing, J.; Botchkarev, V. A.; Pauly-Evers, M.; Saftig, P.; Hafner, A.; Schmidt, P.; Schmahl, W.; Scherer, J.; Anton-Lamprecht, I.; Von Figura, K.; Paus, R.; Peters, C. *FASEB J.* **2000**, *14*, 2075.
9. Pauly, T. A.; Sulea, T.; Ammirati, M.; Sivaraman, J.; Danley, D. E.; Griffor, M. C.; Kamath, A. V.; Wang, I.-K.; Laird, E. R.; Seddon, A. P.; Menard, R.; Cygler, M.; Rath, V. L. *Biochemistry* **2003**, *42*, 3203.
10. Chowdhury, S. F.; Sivaraman, J.; Wang, J.; Devanathan, G.; Lachance, P.; Qi, H.; Ménard, R.; Lefebvre, J.; Konishi, Y.; Cygler, M.; Sulea, T.; Purisima, E. O. *J. Med. Chem.* **2002**, *45*, 5321.
11. Foos, L.; Steel, F.; Rizvi, S. Q. A.; Fraenkel, G. *J. Org. Chem.* **1979**, *44*, 2522.
12. Wakasugi, K.; Nakamura, A.; Iida, A.; Nishii, Y.; Nakatani, N.; Fukushima, S.; Tanabe, Y. *Tetrahedron* **2003**, *59*, 5337.
13. Becker, D. P.; Flynn, D. L. *Synthesis* **1992**, 1080.
14. Irie, O.; Ehara, T.; Iwasaki, A.; Yokokawa, F.; Sakaki, J.; Hirao, H.; Kanazawa, T.; Teno, N.; Horiuchi, M.; Umemura, I.; Gunji, H.; Masuya, K.; Hitomi, Y.; Iwasaki, G.; Nonomura, K.; Tanabe, K.; Fukaya, H.; Kosaka, T.; Snell, C. R.; Hallett, A. *Bioorg. Med. Chem. Lett.* **2008**, *18*, 3959.
15. Altmann, E.; Aichholz, R.; Betschart, C.; Buhl, T.; Green, J.; Irie, O.; Teno, N.; Lattmann, R.; Tintelnot-Blomley, M.; Missbach, M. *J. Med. Chem.* **2007**, *50*, 591.
16. (a) Finlayson, K.; Turnbull, L.; January, C. T.; Sharkey, J.; Kelly, J. S. *Eur. J. Pharmacol.* **2001**, *430*, 147; (b) Snyders, D. J.; Chaudhary, A. *Mol. Pharmacol.* **1996**, *49*, 949.
17. (a) All compounds were characterized by ^{1}H NMR and LC–MS. The experimental information is described in a patent application, see for details: Hart, T. W.; Hallett, A.; Yokokawa, F.; Hirao, H.; Ehara, T.; Iwasaki, A.; Sakaki, J.; Masuya, K.; Kishida, M.; Irie, O. WO 2006018284, 2006.(b) Spectral data of **10b** and **13b**. Compound **10b**: ^{1}H NMR (400 MHz, CDCl$_3$) δ 10.13 (br s, 1H), 7.83 (br s, 1H), 4.38 (d, $J = 6.5$ Hz, 2H), 3.32 (t, $J = 6.3$ Hz, 2H), 2.93 (d, $J = 4.6$ Hz, 3H), 2.97–2.87 (m, 2H), 2.31 (s, 3H), 1.99 (t, $J = 11.0$ Hz, 2H), 1.89–1.56 (m, 13 H), 1.55–1.36 (m, 3H), 1.29–1.17 (m, 2H), 1.09–0.95 (m, 2H). MS (ESI) *m/z* 441 (M+H)$^+$. Compound **13b**: ^{1}H NMR (400 MHz, CDCl$_3$) δ 10.15 (br s, 1H), 8.03 (br s, 1H), 4.64–4.59 (m, 2H), 4.03–3.97 (m, 2H), 3.33 (dd, $J = 6.6$ and 7.1 Hz, 2H), 2.92 (d, $J = 5.0$ Hz, 3H), 1.89–1.58 (m, 11H), 1.53–1.43 (m, 1H), 1.29–1.18 (m, 2H), 1.08–0.96 (m, 2H). MS (ESI) *m/z* 374 (M+H)$^+$. Their purities were greater than 99% by HPLC analysis. The HPLC was performed on analytical Phenomenex C18 Luna 3 μM column (30 × 4.6 mm), gradient 10–100% acetonitrile in water with 0.08% formic acid over 10 min at 3.0 mL/min as the mobile phase. Purity was calculated by integration of UV at 254 nm.
18. (a) Morgan, T. K., Jr.; Sullivan, M. E. *Prog. Med. Chem.* **1992**, *29*, 65; (b) Cavalli, A.; Poluzzi, E.; De Ponti, F.; Recanatini, M. *J. Med. Chem.* **2002**, *45*, 3844.
19. For a recent review, see: (a) Baxter, A. G. *Nat. Rev. Immunol.* **2007**, *7*, 904; (b) Foster, C. A.; Howard, L. M.; Schweitzer, A.; Persohn, E.; Hiestand, P. C.; Balatoni, B.; Reuschel, R.; Beerli, C.; Schwart, M.; Billich, A. *J. Pharmacol. Exp. Ther.* **2007**, *323*, 469.
20. Disease was induced on day 0 by sc injection to SJL/L mice with a mixture of 500 μg bovine MBP in 0.1 ml water emulsified in Freund's complete adjuvant DIFCO (1:1 v/v). On day 9, mice were boosted by re-injection of MBP and an additional iv injection of adjuvant containing *Bordetella pertussis toxin* (200 ng/200 μl saline). An additional injection of the pertussis toxin (125 ng/200 μl) was given on day 11.
21. Clinical grades were as follows: 0, no disease symptoms; 1, loss of tail tonicity; 2, weakness of one of both hind legs and mild ataxia; 3, severe ataxia or paralysis accompanied by urinary incontinence and/or death.